Nucleic Acids Research, 2006, Vol. 34, No. 9 ***2723–2735***
doi:10.1093/nar/gkl348

Human telomeric sequence forms a hybrid-type intramolecular G-quadruplex structure with mixed parallel/antiparallel strands in potassium solution

Attila Ambrus[1], Ding Chen[1], Jixun Dai[1], Tiffanie Bialis[2], Roger A. Jones[3] and Danzhou Yang[1,2,*]

[1]College of Pharmacy, The University of Arizona, 1703 E. Mabel St, Tucson, AZ 85721, USA, [2]Arizona Cancer Center, 1515 N. Campbell Avenue, Tucson, AZ 85724, USA and [3]Department of Chemistry and Chemical Biology, Rutgers University, 610 Taylor Road, Piscataway, NJ 08854, USA

Received March 16, 2006; Revised April 4, 2006; Accepted April 19, 2006

ABSTRACT

Human telomeric DNA consists of tandem repeats of the sequence d(TTAGGG). The formation and stabilization of DNA G-quadruplexes in the human telomeric sequence have been shown to inhibit the activity of telomerase, thus the telomeric DNA G-quadruplex has been considered as an attractive target for cancer therapeutic intervention. However, knowledge of the intact human telomeric G-quadruplex structure(s) formed under physiological conditions is a prerequisite for structure-based rational drug design. Here we report the folding structure of the human telomeric sequence in K^+ solution determined by NMR. Our results demonstrate a novel, unprecedented intramolecular G-quadruplex folding topology with hybrid-type mixed parallel/antiparallel G-strands. This telomeric G-quadruplex structure contains three G-tetrads with mixed G-arrangements, which are connected consecutively with a double-chain-reversal side loop and two lateral loops, each consisting of three nucleotides TTA. This intramolecular hybrid-type telomeric G-quadruplex structure formed in K^+ solution is distinct from those reported on the 22 nt Tel22 in Na^+ solution and in crystalline state in the presence of K^+, and appears to be the predominant conformation for the extended 26 nt telomeric sequence Tel26 in the presence of K^+, regardless of the presence or absence of Na^+. Furthermore, the addition of K^+ readily converts the Na^+-form conformation to the K^+-form hybrid-type G-quadruplex. Our results explain all the reported experimental data on the human telomeric G-quadruplexes formed in the presence of K^+, and provide important insights for understanding the polymorphism and interconversion of various G-quadruplex structures formed within the human telomeric sequence, as well as the effects of sequence and cations. This hybrid-type G-quadruplex topology suggests a straightforward pathway for the secondary structure formation with effective packing within the extended human telomeric DNA. The hybrid-type telomeric G-quadruplex is most likely to be of pharmacological relevance, and the distinct folding topology of this G-quadruplex suggests that it can be specifically targeted by G-quadruplex interactive small molecule drugs.

INTRODUCTION

Telomeres are non-coding highly repetitive sequences at the ends of chromosomes that provide protection against gene erosion at cell divisions, chromosomal non-homologous end-joinings and nuclease attacks (1–3). Telomeric DNA in vertebrates consists of tandem repeats of the sequence d(TTAGGG). Human telomeric DNA is typically 5–8 kb long with a 3′ single-stranded overhang of 100–200 nt (4,5). Each replication results in a 50–200 base loss of the telomere. After reaching a critical shortening of the telomeric DNA, the cell undergoes apoptosis or programmed cell death (6). The structure and stability of telomeres are of great research interest as they are closely related with cancer (7–10), aging (11,12) and genetic stability (3,13,14). The G-rich telomeric sequence can fold into a G-quadruplex, a DNA secondary structure consisting of stacked G-tetrad planes connected by a network of Hoogsteen hydrogen bonds and stabilized by monovalent cations, such as Na^+ and K^+. The formation and stabilization of the DNA G-quadruplex

*To whom correspondence should be addressed. Tel: +1 520 626 5969; Fax: +1 520 626 6988; Email: yangd@pharmacy.arizona.edu

in the human telomeric sequence have been shown to inhibit the activity of telomerase, a cancer-specific reverse transcriptase that is activated in 80–90% of tumors (15). Thus, the telomeric DNA G-quadruplex has been considered to be an attractive target for cancer therapeutic intervention (7,9,10,16–18). More recently, DNA G-quadruplex structures are also found to form in promoter regions of a number of genes functioning as transcriptional regulators (19–28).

Structural information on the intact human telomeric DNA G-quadruplex formed under physiologically relevant conditions is necessary for structure-based rational drug design. Two intramolecular DNA G-quadruplex structures have been reported for the human telomeric sequence using the 22 nt sequence d[AGGG(TTAGGG)$_3$]. Wang and Patel (29) reported a basket-type, mixed antiparallel-parallel stranded G-quadruplex structure in Na^+ solution determined by NMR, which consists of three G-tetrads connected with one diagonal and two lateral (TTA) loops. More recently, Parkinson *et al*. (30) reported a distinctly different propeller-type, parallel-stranded G-quadruplex structure of the same sequence in crystalline state in the presence of K^+, consisting of three G-tetrads connected with three symmetrical double-chain-reversal (TTA) side loops (Figure 1). Because the K^+ structure is considered to be biologically more relevant due to the higher intracellular concentration of K^+, a number of studies have been reported in an attempt to characterize the telomeric G-quadruplex structure in K^+ solution, the results of many of which were inconsistent with the crystal structure (31–37). NMR structure studies have been reported on two dimeric G-quadruplexes of human telomeric sequences in K^+ solution (38,39); however, the intact unimolecular G-quadruplex structure formed in the human telomeric sequence in K^+ solution has yet to be determined.

Here we report the folding structure of the extended four-repeat human telomeric sequence in K^+ solution determined by NMR. Our results demonstrate a novel, unprecedented intramolecular G-quadruplex folding topology with hybrid-type mixed parallel/antiparallel G-strands. This telomeric G-quadruplex structure contains three G-tetrads connected consecutively with a double-chain-reversal side loop and two lateral loops, each consisting of 3 nt TTA. This hybrid-type G-quadruplex structure appears to be the physiologically relevant conformation of the human telomeric sequence. Our results explain all the experimental data reported to date on the human telomeric G-quadruplex formed in the presence of K^+, and provide important insights for understanding the polymorphism and interconversion of various G-quadruplex structures formed within human telomeric sequences, as well as the effects of cations and DNA sequences. Furthermore, this hybrid-type G-quadruplex topology suggests a straightforward path for the secondary structure formation with effective packing within the human telomeric sequence and provides important implications for drug targeting of G-quadruplexes in human telomeres.

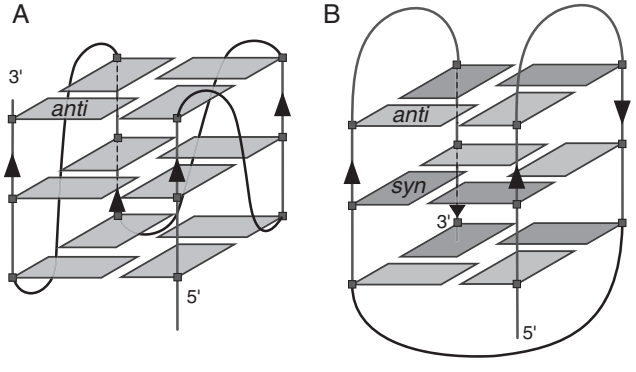

Figure 1. Folding topologies of Tel22. (**A**) Propeller-type parallel-stranded intramolecular G-quadruplex in the presence of K^+ in crystalline state. (**B**) Basket-type mixed parallel/antiparallel-stranded intramolecular G-quadruplex in Na^+ solution determined by NMR.

MATERIALS AND METHODS

Chemicals

All chemicals were from Sigma if not stated otherwise.

DNA sample preparation

The DNA oligonucleotides were synthesized on solid-phase and purified by high-performance liquid chromatography as described previously (40–42). 1,2,7-^{15}N, 2-^{13}C guanine phosphoramidite was synthesized as reported previously (43) and was applied for site-specific ^{15}N, ^{13}C-labeling of DNA in 6% low-level enrichment. Samples in D_2O were prepared by repeated lyophilization and final dissolution in 99.96% D_2O while water samples were prepared in 5%/95% D_2O/H_2O. The final NMR samples contained 0.1–3.5 mM DNA oligonucleotides in 25 mM K-PO_4 and 70 mM KCl, pH 7.0.

NMR experiments

NMR experiments were performed on a Bruker DRX-600 spectrometer. Identifications of guanine H1 protons of site-specific labeled oligonucleotides were performed by 1D JR-HMQC using the jump-and-return sequence for water suppression (40,42,44,45). H1–H8 intra-residual connectivities (through the C5 atom) were determined in a natural abundance JR-HMBC experiment (46). Standard homonuclear 2D NMR experiments, including COSY, TOCSY and NOESY, were used to assign the non-exchangeable proton chemical shifts in D_2O at 1, 7, 15 and 25°C. The 2D NOESY experiments for H1/H1 and H1/H8 correlations were recorded in H_2O using jump-and-return water suppression at the same temperatures. A variable temperature study of 1D ^{1}H spectra was recorded in H_2O at 2.5 mM concentration from 7 to 85°C. At the determined melting point (55°C), stoichiometric titration of the melted and the folded strands as a function of total strand concentration was performed from 0.1 to 0.3 mM. A D-to-H exchange time-course experiment was recorded for nine time-points for 3.5 h at 2.5 mM strand concentration. Peak assignments were achieved using Sparky (UCSF).

CD spectroscopy

CD spectra of the oligonucleotides were recorded on a Jasco J-810 spectropolarimeter (Jasco, Easton, MD). A quartz cell of 1 mm optical path length and an instrument scanning speed of 100 nm/min with 1 s response time was used for measurements. The measurements are the averages of three

repetitions between 200 and 320 nm at room temperature. Spectra were baseline-corrected and the signal contributions of the buffer were subtracted. DNA solutions for CD measurements were generally diluted with H_2O or appropriate buffer from pre-tested (NMR) samples [in 25 mM K(/Na)-PO_4, 70 mM K(/Na)Cl, pH 7.0] to 20–40 μM strand concentrations. Titrations were performed by high concentration stock solutions of NaCl or KCl.

RESULTS

A human telomeric sequence that forms a single intramolecular G-quadruplex structure in K^+ solution

To date the 22 nt human telomeric sequence of d[AGGG-$(TTAGGG)_3$] (Tel22) (Figure 2A) has been used for all structural studies on unimolecular G-quadruplex structure formed within the human telomeric sequence (29,30). This sequence forms a single stable basket-type unimolecular G-quadruplex in the presence of Na^+; however, it appears to form a mixture of multiple G-quadruplex conformations in the presence of K^+, as indicated by 1D NMR spectra (Figure 2C).

The Tel22 is a truncated human telomeric sequence with no 3′-flanking sequence. It has been shown that flanking sequences of a quadruplex-forming sequence can be very important in stabilizing the formation of a stable G-quadruplex structure (42,47), therefore this insight was employed in searching for a proper candidate for the human telomeric sequence which would form a single stable unimolecular G-quadruplex structure in the presence of K^+. We have tested >20 different combinations of flanking sequences on the 22 nt human telomeric sequence Tel22. Several sequences are found to form a stable major G-quadruplex conformation in the presence of K^+ (Supplementary Figure S1); in fact, it appears that the 3′-flanking sequence is critical for the formation of a stable G-quadruplex structure in K^+. The 26 nt four repeat telomeric sequences with one or two adenine(s) at each end give rise to the same clean NMR spectra (Supplementary Figure S1). Among them, a 26 nt sequence Tel26 (Figure 2A) gave a well-resolved NMR spectrum, with spectral characteristics similar to that of the wild-type four repeat 26 nt telomeric sequence (WT-Tel26) (Figure 2A and Supplementary Figure S1), and was selected for further NMR structural analysis. The sequence of this Tel26 is very similar to that of WT-Tel26 (Figure 2A), with the only difference being the two bases in the flanking sequence at each end. Significantly, the CD spectra of WT-Tel26 and Tel26 are very similar and exhibit the same signature profiles, suggesting strongly that they both adopt the same major conformation in K^+ solution (Figure 3). The CD signature of Tel26 and WT-Tel26 is clearly different from those of the Na^+ forms and of the Tel22 in K^+ (Figure 3).

The 1D ^{1}H NMR spectrum of the Tel26 sequence in K^+ solution shows 12 well-resolved imino proton resonances at 10.5–12 ppm with sharp line widths (~6 Hz at 25°C) (Figure 2B), clearly indicating the formation of a predominant unimolecular G-quadruplex structure. Minor conformations are also present as indicated by the presence of weak resonances, whose intensities are <5% of the major species

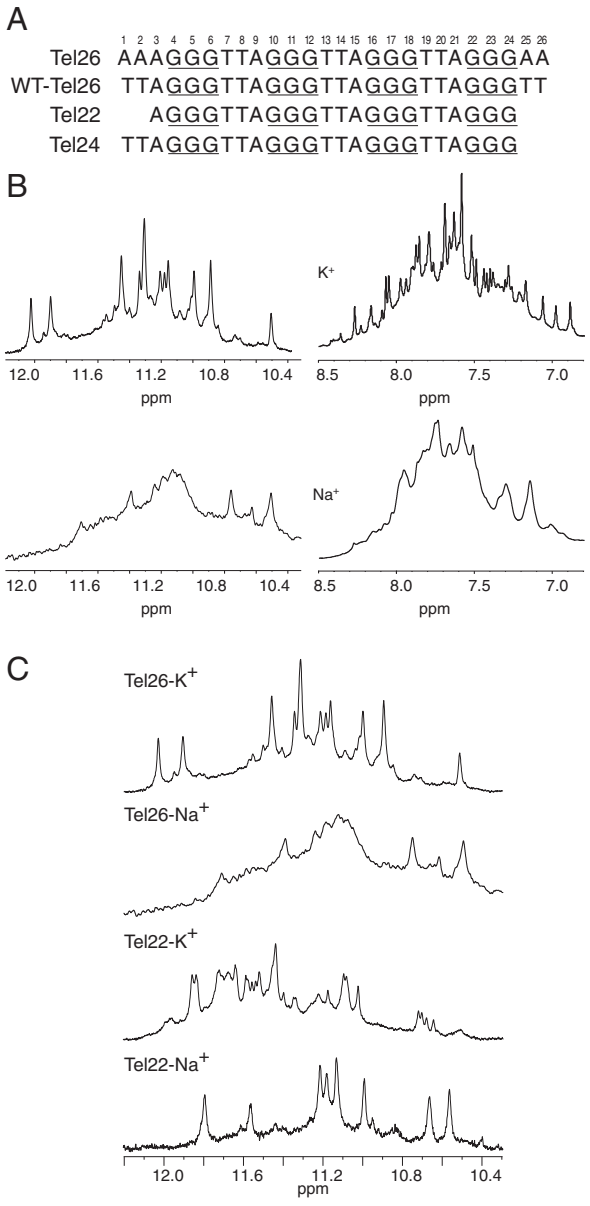

Figure 2. (**A**) Different four repeat telomeric DNA sequences. WT-Tel26, Tel22 and Tel24 are the wild-type four repeat telomeric DNA sequences with sizes of 26, 22 and 24 nt, respectively. The numbering system is shown above Tel26. (**B**) Imino and aromatic regions of 1D ^{1}H NMR spectra of Tel26 in K^+ and Na^+ solutions at 25°C. (**C**) Imino regions of 1D ^{1}H NMR spectra of Tel22 and Tel26 in Na^+ and K^+ solutions at 25°C.

and thus do not interfere with the unambiguous structural analysis of the predominant telomeric G-quadruplex structure. The proton NMR spectrum of the Tel26 in the presence of K^+ is clearly different from that of the Tel22 sequence in the presence of Na^+ (Figure 2C). The formation of a unimolecular structure is confirmed by the NMR stoichiometry titration experiment (45) and electrophoretic mobility shift assay (Supplementary Figure S2). In addition, the melting temperature of this G-quadruplex appears to be concentration-independent, as shown by NMR and CD data, which is also in accord with the presence of a unimolecular structure. The NMR spectra of Tel26 at a strand

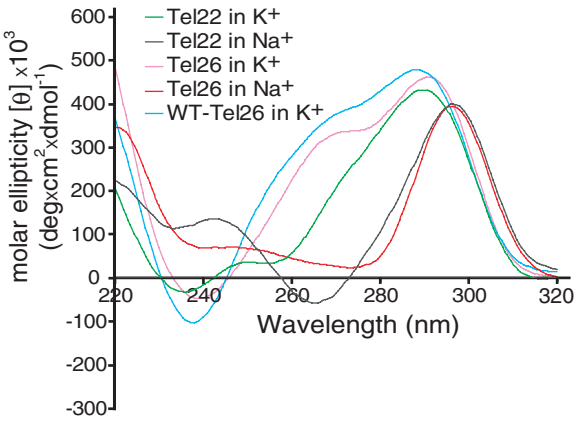

Figure 3. CD spectra of Tel26, WT-Tel26 and Tel22 in 100 mM Na^+ or K^+ solutions at 25°C. The same CD signatures are observed for Tel26 and WT-Tel26 in K^+ solution, while similarly distinct CD signatures are observed for Tel22 and Tel26 in Na^+ solution.

concentration of 2.5 mM (for 2D NMR experiments) and 0.6 mM (for 1D experiments) are the same (Supplementary Figure S3), indicating the same unimolecular G-quadruplex structure is formed in all the conditions used for our NMR analysis.

In contrast to the Tel22 sequence that has been used for all the structural studies of the telomeric G-quadruplex to date (29,30), both the Tel26 and WT-Tel26 sequences do not form a well-defined unique G-quadruplex structure in the presence of Na^+, as indicated by broad envelopes in 1D ^1H NMR (Figure 2B and Supplementary Figure S1).

Assignment of guanine proton resonances of the Tel26 G-quadruplex in K^+

The presence of 12 imino peaks in the 1D proton spectrum of Tel26 in K^+ (Figure 2B) indicates that all 12 guanines are involved in the intramolecular G-quadruplex formation, and that this G-quadruplex structure contains 3 G-tetrads. The imino and base aromatic H8 protons of 12 guanine residues have been unambiguously assigned by site-specific low-enrichment (6%) using 1,2,7-^{15}N, 2-^{13}C-labeled guanine nucleoside at each guanine position of the sequence (40,42). The guanine imino H1 proton resonance has one-bond coupling to N1, and the guanine base aromatic H8 proton resonance has two-bond coupling to N7. Both H1 and H8 protons of the site-specific labeled guanine are readily detected by 1D ^{15}N-filtered experiments. The assignment of each imino proton H1 of the 12 guanines involved in the three G-tetrads is shown in Figure 4A. The assignment of guanine H1 and H8 protons is further confirmed by the long-range HMBC experiment (Figure 4B). The base H6 proton resonances of thymines have been unambiguously assigned by substituting deoxyuridine (dU) for dT at each thymine position of the Tel26 sequence one at a time. Complete assignment of the proton resonances of Tel26 was accomplished by using 2D-NOESY, TOCSY and COSY data, and the standard DNA sequential assignment procedure (Supplementary Figure S4). The glycosidic torsion angles of five G-quadruplex guanines are in the *syn* conformation, including G4, G10, G16, G17, G22, as indicated by the very strong intraresidue H8–H1′ NOE intensities (Supplementary Figure S4).

Folding structure of the Tel26 G-quadruplex structure in K^+

The assignment of the imino and base H8 protons of guanines leads to the direct determination of the folding topology of the telomeric G-quadruplex structure in K^+ solution. In a G-tetrad plane with the Hoogsteen H-bond network, the imino proton NH1 of each guanine is in close spatial vicinity to the NH1s of the two adjacent guanines, and to the base H8 of one of the adjacent guanines (Figure 5A). The through-space NOE connectivities of guanine H1–H1 and H1–H8 (Figure 6) determine the arrangement and topology of a G-tetrad plane. Three G-tetrad planes were determined based on the NOE connectivities (Figure 5B). For example, the GH1/GH1 NOE interactions, including G5H1/G11H1, G11H1/G17H1, G17H1/G23H1 and G23H1/G5H1 (Figure 6), and the GH1/GH8 NOE interactions, including G5H1/G11H8, G11H1/G17H8, G17H1/G23H8 and G23H1/G5H8 (Figure 6), define a G-tetrad plane of G5–G11–G17–G23. Using the same method, two other G-tetrad planes, G4–G10–G18–G22 and G6–G12–G16–G24, were also defined (Figure 5B). The overall G-quadruplex alignment is further defined based on the inter-tetrad NOE connections from residues that position far apart in DNA sequence. For example, the strong NOE interactions of G4H1/G23H1, G22H1/G17H1, G18H1/G11H1 and G5H1/G10H1 (Figure 6) connect the top and middle G-tetrad planes, as well as reflecting the different G-arrangement with the reversed glycosidic conformations of guanines of the top two tetrad planes (Figure 5B). The sequential NOE interactions, including G5H1/G6H1, G11H1/G12H1, G16H1/G17H1 and G23H1/G24H1 (Figure 6) indicate the same G-arrangement and glycosidic conformations (*syn–syn* or *anti–anti* steps) of the middle and bottom G-tetrad planes, while the inter-residue NOEs between the two G-tetrad planes, e.g. G6H1/G11H8, G12H1/G17H8, G16H1/G23H8 and G24H1/G5H8 (Figure 6), reflect the right-handed twist of the DNA backbone. From these data, the folding topology of the Tel26 G-quadruplex was unambiguously determined, which is shown in Figure 5B. The NOE connectivities used to determine the folding topology of Tel26 G-quadruplex are summarized in Supplementary Figure S5.

The telomeric G-quadruplex adopts a novel folding topology. The telomeric G-quadruplex is a hybrid-type mixed parallel/antiparallel-stranded G-quadruplex structure, with the first, second and fourth G-strands being parallel with each other, and the third G-strand being antiparallel with the other three strands. The first two G-strands (from the 5′ end) are linked with a double-chain-reversal TTA side loop, while the second, third and fourth strands are linked with two TTA lateral loops. The bottom two G-tetrads have the same *anti*/*syn* distribution and are connected by guanines with the same sugar glycosidic conformations, while the first G-tetrad has a reversed *anti*/*syn* distribution and is connected with the middle G-tetrad by guanines with reversed sugar glycosidic conformations (Figure 5B).

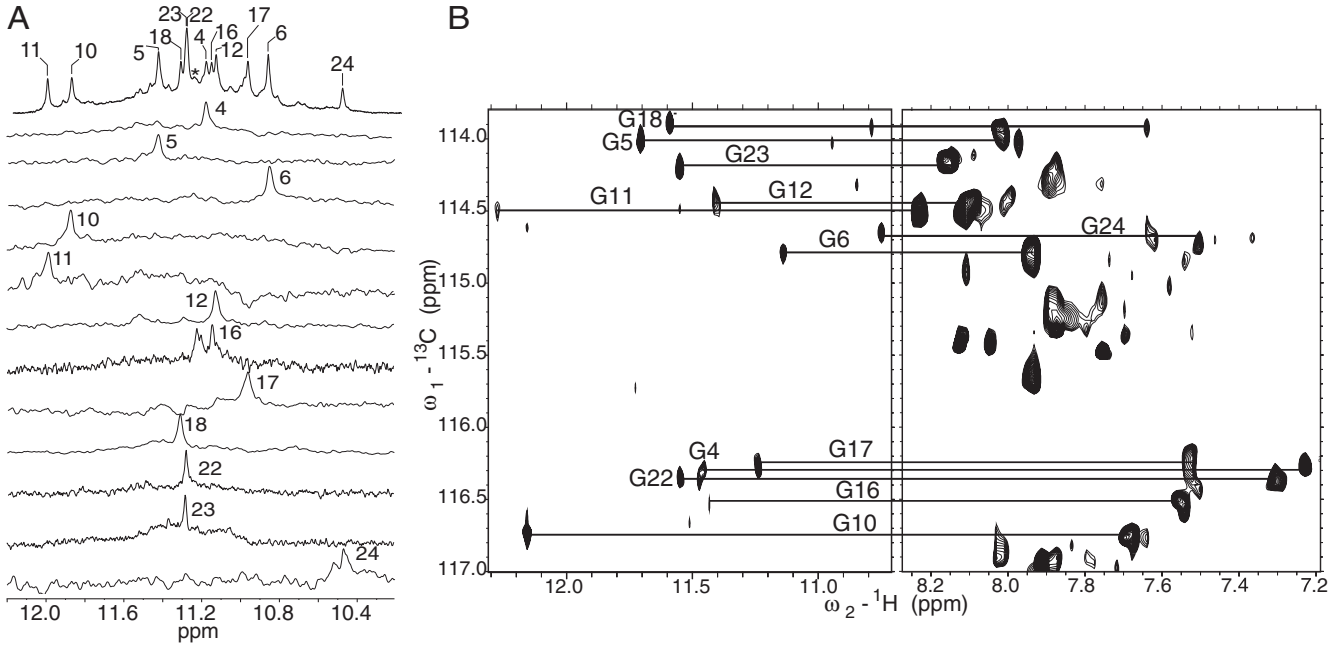

Figure 4. (**A**) Imino proton assignments of Tel26 using 1D ^{15}N-filtered experiments on site-specific labeled oligonucleotides. Conditions: 25 mM K-PO_4, 70 mM KCl, pH 7.0, 25°C, 0.6–0.7 mM DNA. (**B**) Long-range through-bond correlations between intraresidue imino and H8 protons via C5 of the guanine base, determined by JR-HMBC experiment at natural abundance (46).

NMR spectroscopic studies of various telomeric sequences

We have carried out systematic analysis of various telomeric sequences to obtain insights on G-quadruplex structure stabilization and the effect of K^+ and Na^+ cations. The 1D ^{1}H NMR spectra of Tel26 and Tel22 in the presence of either K^+ or Na^+ are shown in Figure 2C. The Tel26 sequence forms a well-defined intramolecular G-quadruplex structure (hybrid-type) in the presence of K^+, as indicated by a well-resolved NMR spectrum (Figure 2C); however, it does not form a well-defined G-quadruplex structure in the presence of Na^+, as shown by broad envelopes in 1D NMR with some fine lines (Figure 2C). In contrast, the truncated Tel22 sequence in the presence of Na^+ forms a single intramolecular G-quadruplex structure, with distinct chemical shifts of imino protons from those of Tel26 in K^+, corresponding to the different basket-type of structure (Figure 2C). However, the Tel22 sequence does not form a single G-quadruplex structure in the presence of K^+, as indicated by the much larger number of G-quadruplex imino peaks in the characteristic region of 10.5–12 ppm (Figure 2C). Interestingly, the relatively sharp lines of proton peaks in 1D NMR of Tel22 in K^+ indicate the presence of stable, but multiple, G-quadruplex conformations (Figure 2C). The 1D NMR spectra of various telomeric sequences containing different combinations of flanking sequences on the Tel22 sequence are shown in Supplementary Figure S1.

CD spectroscopic profiles of different telomeric G-quadruplex structures

The CD spectra of Tel26 and Tel22 in the presence of K^+ and Na^+ are shown in Figure 3. CD has become a very useful technique for the characterization of G-quadruplex-forming oligonucleotides. Signature spectra have been reported for many G-quadruplex structures based on the orientation of the DNA strands and thus the resulting different stacking of guanine residues (48,49). Guanines in the parallel-stranded G-quadruplex all have the same *anti* glycosidic conformation, exhibiting a positive peak at 260 nm and a small negative peak at 240 nm in CD spectra, such as those observed in the c-Myc promoter G-quadruplex (50). In contrast, guanines in the antiparallel-stranded G-quadruplex have alternating *anti* and *syn* glycosidic conformations along each DNA strand, exhibiting a characteristic positive peak at 295 nm, a smaller negative peak at 265 nm, and a smaller positive peak at 245 nm in CD spectra (48). This characteristic CD spectrum is indeed observed for Tel22 in Na^+ (Figure 3), which forms a basket-type G-quadruplex structure containing G-strands with alternating guanine glycosidic conformations (Figure 1). The same CD signature has also been reported for the chair-type G-quadruplex formed in a thrombin-binding aptamer (48,50), which also contains DNA G-strands with alternating glycosidic conformations (51). Another truncated human telomeric sequence lacking the 3′-flanking sequence, Tel24 (Figure 2A), has also been reported to give rise to a similar CD signature in K^+ solution (32,37,52). In contrast, the Tel26 sequence in the presence of K^+, which forms a well-defined hybrid-type G-quadruplex (Figure 5B), exhibits a distinct CD spectrum containing a strong positive peak around 290 nm with a shoulder peak around 268 nm, and a smaller negative peak at 240 nm (Figure 3). The strong positive peak around 290 nm is likely due to the alternating guanine glycosidic conformations along G-strands between the top and middle G-tetrads in the hybrid-type telomeric G-quadruplex (Figure 5B), and its shifting from 295 nm is

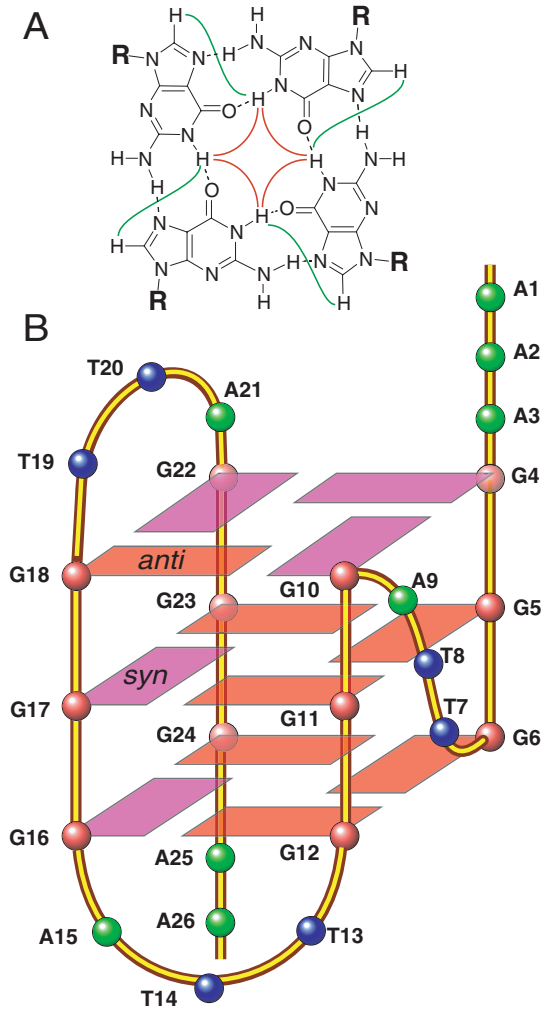

Figure 5. (**A**) A G-tetrad with H1–H1 and H1–H8 connectivity patterns detectable in NOESY experiments. (**B**) Schematic diagram of the folding topology of the unimolecular human telomeric G-quadruplex in K^+ solution. red ball, guanine; red box, (*anti*) guanine; magenta box, (*syn*) guanine; green ball, adenine; blue ball, thymine.

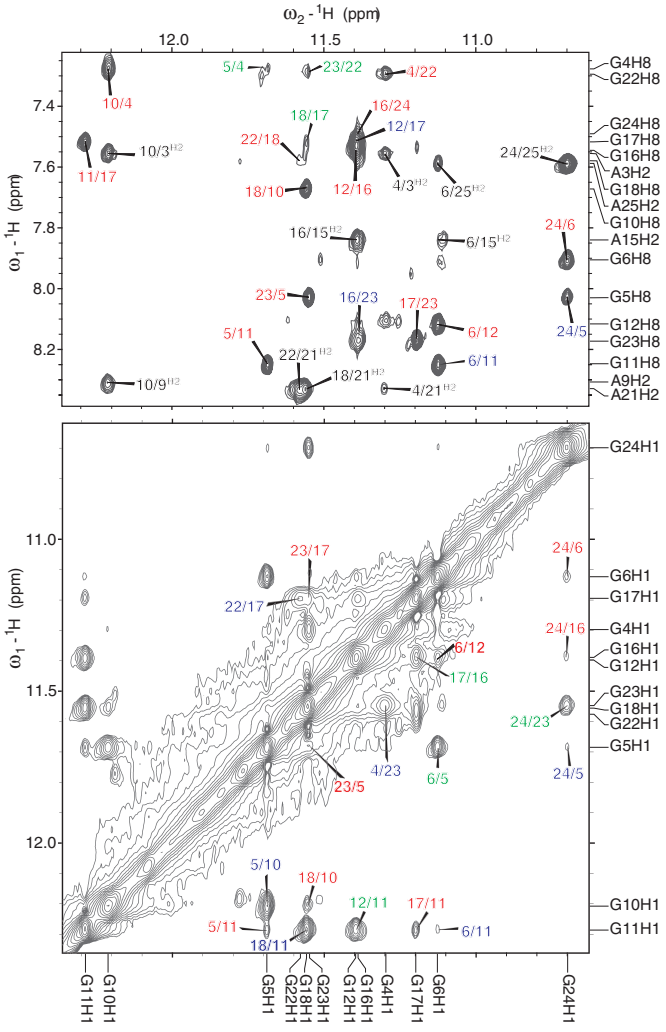

Figure 6. The expanded H1–H8/H2/H6 and H1–H1 regions of the exchangeable proton 2D JR-NOESY spectrum of Tel26 in K^+ solution at 1°C. NOEs are labeled as follows: intra-tetrad NOEs are labeled in red, sequential NOEs are labeled in green, inter-tetrad NOEs are labeled in blue, NOEs between stacking adenine H2 protons and G-tetrad imino protons are labeled in black. Conditions: 1°C, 25 mM K-PO_4, 70 mM KCl, pH 7.0, 2.5 mM DNA.

probably due to the presence of the positive peak at 260 nm. The positive peak around 265 nm (shifted to a longer wavelength from 260 nm due to the presence of the positive peak at 290 nm) and the smaller negative peak around 240 nm are likely from the non-alternating guanine glycosidic conformations between the middle and bottom G-tetrads. The wild-type 26 nt telomeric sequence shows a very similar CD spectrum to that of Tel26 in the presence of K^+ (Figure 3), strongly indicating that the hybrid-type G-quadruplex is likely to be the major conformation for the wild-type 26 nt telomeric sequence as well.

The CD spectrum of Tel26 in the presence of Na^+ is quite similar to that of Tel22, with some changes in the region of 230–280 nm, indicating the formation of the basket-type G-quadruplex structure, although it is not as well-defined as indicated by the lack of well-resolved peaks in the NMR spectrum (Figure 2B). Interestingly, the Tel22 sequence in the presence of K^+ gives rise to a CD spectrum with a strong positive peak at 290 nm, a much smaller shoulder at 265 nm and a smaller negative peak at 235 nm (Figure 3), which can be considered as a summation spectrum of multiple G-quadruplexes, such as the hybrid-type Tel26/K^+ form G-quadruplex and the basket-type Tel22/Na^+ form G-quadruplex. It is noteworthy that the basket-type G-quadruplex and the chair-type G-quadruplex give rise to very similar CD spectra (48,50). This is in accord with the previously discussed NMR data for Tel22 in K^+ (Figure 2B), which indicates the presence of more than one stable G-quadruplex conformations.

Interconversion of telomeric G-quadruplexes formed in K^+ and Na^+

To examine the interconversion and stability of the two G-quadruplex conformations formed in the presence of K^+ or Na^+, we have carried out cation titration studies using CD spectroscopy. The Tel26 sequence was first incubated in the

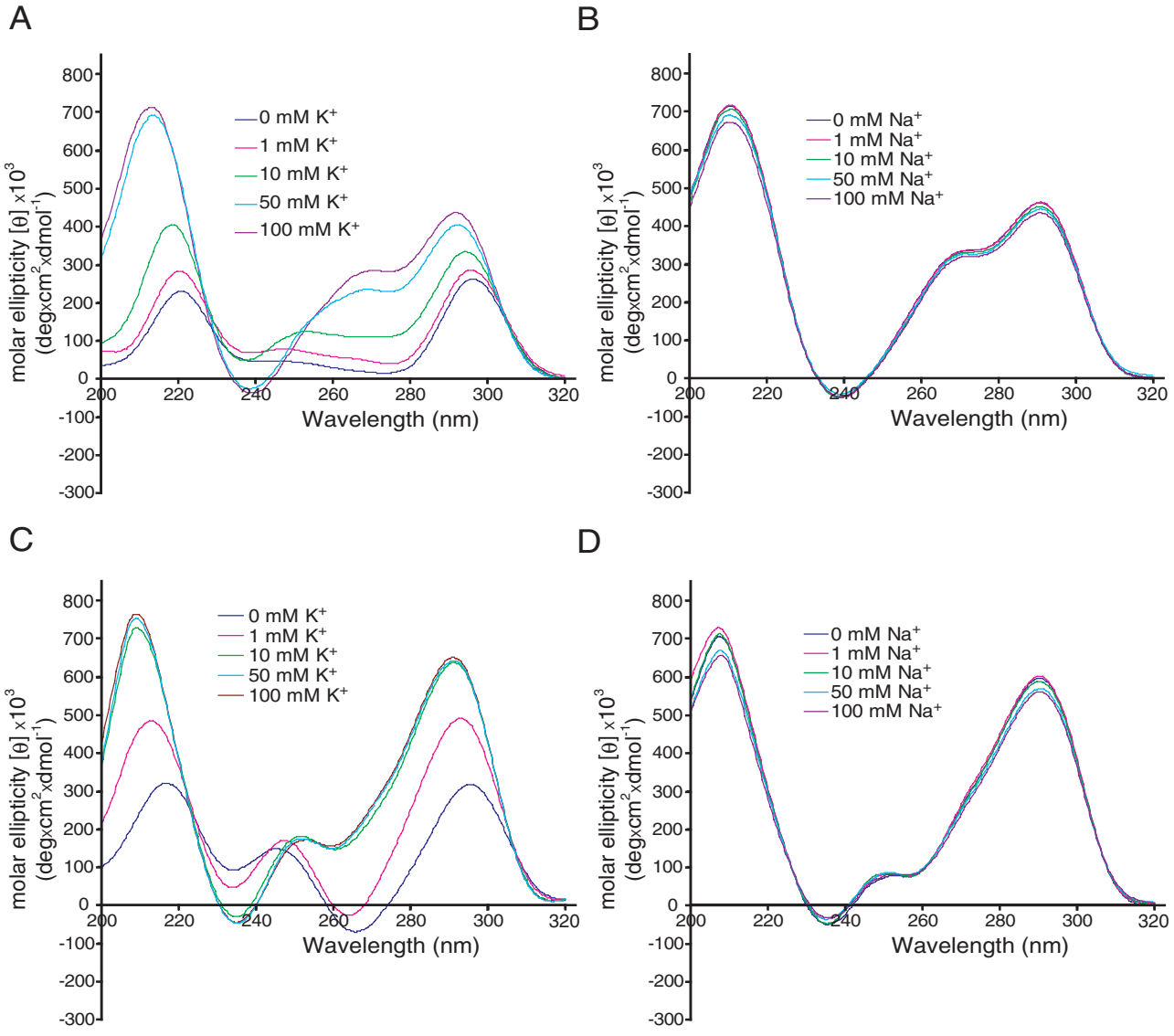

Figure 7. Titration experiments of K^+ in the presence of 150 mM Na^+ for Tel26 (**A**) and Tel22 (**C**), and titration experiments of Na^+ in the presence of 100 mM K^+ for Tel26 (**B**) and Tel22 (**D**), monitored by CD spectroscopy.

presence of 100 mM Na^+ to form the basket-type Na^+ G-quadruplex structure as indicated by CD spectrum, and then K^+ was gradually added into the preformed Tel26/Na^+ G-quadruplex for CD measurements without allowing any equilibration time. Clear spectral changes were observed from the first addition (Figure 7A), indicating the conversion of the basket-type Tel26/Na^+ G-quadruplex to the hybrid-type Tel26/K^+ G-quadruplex conformation. We have also tried incubating the Tel26 sequence with lower levels of K^+ to see if Na^+ would then have an effect on the structure. An overnight incubation of 10 mM K^+ in the presence of 100 mM Na^+ results in a CD spectrum fairly similar to that of 100 mM K^+ (Supplementary Figure S6), indicating that Na^+ does not affect the structure even at the low K^+ concentration. In contrast, addition of Na^+ into the preformed Tel26 hybrid-type G-quadruplex with the preincubation of 100 mM K^+ does not induce any spectral change (Figure 7B). Therefore, the hybrid-type telomeric G-quadruplex structure is a more stable, and thus the predominant, conformation for Tel26 in the presence of K^+, regardless of the presence or absence of Na^+. Interestingly, the same results are also observed for the truncated Tel22 sequence (Figure 7C and D), in that the addition of K^+ can convert the basket-type G-quadruplex to the K^+ conformation in the presence of Na^+, while the addition of Na^+ does not have any effect on the K^+ G-quadruplex conformation.

Full conversion of the Na^+ form of Tel26 to its K^+ form takes several hours to an overnight incubation depending on the K^+ concentration, as indicated by the CD experiments (Figure 7A and Supplementary Figure S6) and the empirical observation in NMR experiments. In contrast, conversion of the Na^+ form of Tel22 to its K^+ form is faster than can be

detected by either CD or NMR (Figure 7C), and the related equilibrium occurs in minutes at a given Na^+/K^+ concentration ratio.

Stability of the hybrid-type K^+ telomeric G-quadruplex structure

The melting profile of the Tel26/K^+ G-quadruplex structure was examined at variable temperatures using CD and NMR spectroscopic methods (Figure 8 and Supplementary Figure S7). Both studies indicate a melting temperature around 55°C for this G-quadruplex structure. The D_2O-to-H_2O exchange experiments by 1D proton NMR for Tel26 are shown in Figure 8B. In accord with the folding topology, the imino protons of the middle G-tetrad, including G5, G11, G17 and G23, which are less accessible to solvent, are slower to exchange from D_2O to H_2O and therefore are the last to appear.

DISCUSSION

Folding topology of the telomeric G-quadruplex structure in K^+

The 26 nt telomeric sequence Tel26 in the presence of K^+ forms a single intramolecular G-quadruplex that adopts a novel hybrid-type folding topology, which to the best of our knowledge is the first example of this folding topology. It is significant to note that the G-quadruplex structure formed on the 26 nt Tel26 in K^+ solution is distinct from those reported on the 22 nt Tel22 in Na^+ solution (29) and in crystalline state in the presence of K^+ (30). The telomeric G-quadruplex in K^+ solution adopts a hybrid-type mixed parallel/antiparallel-stranded G-quadruplex structure, with the first, second and fourth G-strands being parallel with each other, and the third G-strand being antiparallel with the other three strands. The first two G-strands (from the 5′ end) are linked with a double-chain-reversal TTA side loop, while the second, third and fourth strands are linked with two TTA lateral loops (Figure 5B). The three G-tetrads have mixed G-arrangements, with the top G-tetrad being (*syn:syn:anti:syn*) and the bottom two being (*anti:anti:syn:anti*); thus the hybrid-type telomeric G-quadruplex contains guanines with alternating glycosidic conformations between the top two G-tetrads along each G-strand (Figure 5B).

Comparison of the available G-quadruplex structures provides insights into the rules governing various folding patterns of intramolecular G-quadruplexes. Interestingly, the recently determined G-quadruplex formed in the bcl-2 promoter (40) (Figure 9), and the G-quadruplex formed in the *Tetrahymena* telomeric sequence in Na^+ solution (53), also adopt mixed parallel/antiparallel-stranded structures with a different hybrid-type folding containing a different order of loop conformations, which from the 5′ end are consecutively lateral, lateral and double-chain-reversal. Another G-quadruplex structure formed in the c-Myc promoter has also been determined recently by our lab (42), adopting a parallel-stranded folding with three double-chain-reversal side loops of 1 or 2 nt sizes (Figure 9). A mutant c-MYC promoter sequence, c-MYC(b), whose central Gs are mutated to Ts, adopts a parallel-stranded folding as well (47) (Figure 9). However, the bcl-2 promoter sequence, which exhibits apparent sequence similarity to c-MYC(b) with one notable difference in the 5′ end loop region, wherein the bcl-2 sequence contains 3 nt instead of 1 nt, adopts a hybrid-type mixed parallel/antiparallel-stranded folding. The 5′ end 3 nt loop in the bcl-2 promoter sequence forms a lateral loop, as opposed to a double-chain-reversal loop in the mutant c-MYC(b), and appears to largely determine the overall folding of the bcl-2 G-quadruplex. It is thus important to note that the 1 nt double-chain-reversal loop, as found in the bcl-2 and c-MYC promoter G-quadruplexes (40,42,47,50) (Figure 9), and in a number of other DNA sequences (54–56), is very stable and provides a robust parallel-stranded structural motif. Moreover, it appears that a longer (3 nt sized) loop is not as favored for the formation of the double-chain-reversal loop conformation, probably owing to the lack of stacking interactions of the residues in the side loop. This may explain why the human telomeric sequence does not form a stable parallel-stranded G-quadruplex in solution, as an intramolecular G-quadruplex structure with three 3 nt double-chain-reversal side loops is unlikely to be stable. Furthermore, the hybrid-type folding can be the most-favored one for non-parallel-stranded intramolecular G-quadruplexes with extended flanking sequences, because the extended 5′ and 3′ ends are pointing into opposite directions and thus will not have any steric interference. This may be the reason for the presence of a 3 nt double-chain-reversal loop in the hybrid-type telomeric K^+ G-quadruplex even though it is not the most energy-favorable conformation by itself. Indeed, the other two non-parallel-stranded intramolecular G-quadruplex foldings, including the basket-type and chair-type structures, both have the 5′ and 3′ ends positioned on the same side of the G-quadruplexes and are all observed in DNA sequences with no or 1 nt flanking sequences (29,51,57).

The extended human telomeric sequence Tel26 forms a stable intramolecular structure in K^+ solution, but not in Na^+ solution

The extended 26 nt telomeric sequence Tel26 forms a well-defined unique intramolecular hybrid-type G-quadruplex in K^+ solution. Moreover, it appears that the 3′-flanking sequence is critical for the formation of a stable intramolecular G-quadruplex structure in the human telomeric sequence in K^+ (Supplementary Figure S1), such as in the Tel26 sequence used for our NMR structural analysis. However, even though the CD spectrum shows the formation of a basket-type G-quadruplex in Na^+ solution (Figure 3), Tel26 no longer forms a well-defined intramolecular G-quadruplex structure in Na^+ solution as indicated by broad envelopes in 1D NMR (Figure 2B). This result indicates that the 3′-flanking sequence in the Tel26 sequence destabilizes the basket-type G-quadruplex structure in Na^+ solution, which is likely caused by the steric interference of the 3′-flanking sequence with the diagonal loop, both of which are positioned on the same side of the basket-type G-quadruplex structure (Figure 10A).

Significantly, the hybrid-type G-quadruplex structure appears to be the most stable conformation for Tel26 in the presence of K^+, regardless of the presence or absence of

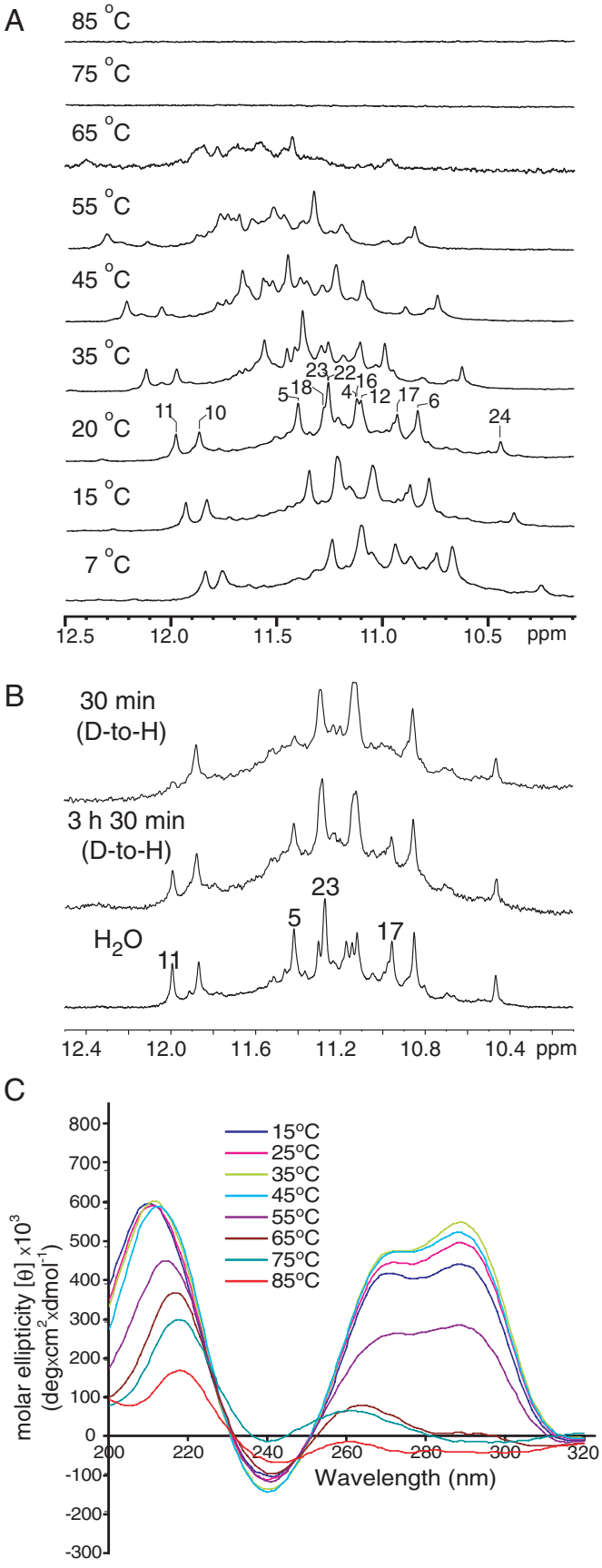

Na^+. The basket-type telomeric G-quadruplex conformation formed in Na^+ solution is not favored in the presence of K^+. CD studies show that addition of K^+ readily converts the preformed Na^+-form G-quadruplex to the hybrid-type G-quadruplex conformation (Figure 7A). Concentrations as low as 10 mM of K^+ can stabilize the major hybrid-type conformation in the presence of 100 mM Na^+ (Supplementary Figure S6). In contrast, addition of Na^+, even to a concentration of 200 mM, does not convert the hybrid-type telomeric G-quadruplex formed in K^+ solution to the basket-type conformation (Figure 7B). These results indicate that the hybrid-type telomeric G-quadruplex is the predominant form in the presence of K^+, even in the co-presence of a high concentration of Na^+ (Figure 10A). Complete conversion of the Na^+ form of Tel26 to its K^+ form takes a considerable amount of time as indicated by the CD experiments (Figure 7A and Supplementary Figure S5) and the empirical observation in NMR experiments. Both techniques show that the completely equilibrated final K^+ form of Tel26 (starting from H_2O or Na^+ solution) appears only after several hours to an overnight incubation depending on the K^+ concentration.

The CD spectrum of Tel26 in K^+ solution, which has been shown by NMR to adopt a unimolecular hybrid-type G-quadruplex, is clearly from a predominant single G-quadruplex structure. The CD signature of a well-defined structure can be used to demonstrate the presence of the structure in a not-so-well-defined system, which has been reported in many studies with a few examples referenced here (48,50,56,58). The fact that the CD spectrum of WT-Tel26 is very similar to that of Tel26, which is clearly different from that of Tel22 in K^+ that arises from multiple different conformations, strongly suggests that the hybrid-type G-quadruplex formed in Tel26 is the major conformation formed in WT-Tel26 in K^+.

The truncated Tel22 sequence in K^+ solution likely forms multiple G-quadruplex conformations, which are interconvertable

The truncated 22 nt telomeric sequence Tel22, which has been used for all the structural analyses of intramolecular human telomeric G-quadruplexes (29,30), forms a well-defined basket-type intramolecular G-quadruplex structure in the presence of Na^+ (Figure 2C). However, this Tel22 sequence does not form a single G-quadruplex structure in the presence of K^+ as indicated by the number of imino proton peaks in the 1D NMR spectra (Figure 2C). Interestingly, the NMR peaks observed for the Tel22 sequence in K^+ are relatively sharp, unlike those of Tel26 in Na^+ solution, indicating the presence of multiple stable G-quadruplex conformations in K^+ solution. This is also supported by the CD

Figure 8. (**A**) Imino proton region of Tel26 in K^+ solution in a variable temperature study. As seen above 65°C there is no detectable peak intensity in the imino (exchangeable proton) region. The imino protons are labeled on the spectrum recorded at 20°C. (**B**) D_2O-to-H_2O NMR exchange experiments. The imino region of the 1D ^1H NMR spectrum of Tel26, which was first incubated overnight in 99.96% D_2O and then incubated in H_2O for 30 min, 3.5 h and then overnight at 25°C. Imino protons from the middle layer of the G-tetrad (Figure 5) are the last to appear and are labeled with the residue numbers. (**C**) Melting profile of Tel26 in K^+ solution in a CD variable temperature study. The same melting temperature of 55°C is shown by both CD and NMR (A).

Figure 9. Comparison of G-quadruplex-forming sequences. Loops colored in red have been shown to adopt parallel-stranded double-chain-reversal side loops (for more details see text).

data, as the CD spectrum of Tel22 in K^+ can be considered as the sum of the CD spectrum of hybrid-type G-quadruplex and the CD spectrum of basket-type G-quadruplex (Figure 3). It is noteworthy that the basket-type G-quadruplex and the chair-type G-quadruplex give rise to very similar CD spectra. Therefore, the truncated Tel22 sequence is likely to have two stable G-quadruplex conformations (possible hybrid-type and basket-type) co-existing in the presence of K^+ (Figure 10B), and the exchange rate between the different G-quadruplexes is in the slow-exchange regime on the NMR time scale, as they are shown in NMR spectra as separate sharp peaks. Close examination of the folding topologies of the hybrid-type and basket-type telomeric intramolecular G-quadruplexes reveals a possible mechanism of the interconversion of the two telomeric G-quadruplex conformations of the Tel22 sequence in K^+ solution. As shown in Figure 10B, the first G-strand of the basket-type G-quadruplex may dissociate from the structure and swing back to the other side of the second G-stand to form a parallel-stranded structural motif with a double-chain-reversal loop. The first two G-tetrad planes do not need to be completely melted for the new conformation as the other six guanines still keep the same relative positions and glycosidic sugar conformations, while the bottom G-tetrad is likely to be melted and dissociated to rearrange the guanine conformation.

In accord with the extended Tel26 sequence, addition of K^+ to the preformed basket-type G-quadruplex structure of the Tel22 sequence (in the presence of 100 mM Na^+) readily converts the G-quadruplex conformation to the K^+-form as shown by the CD spectroscopic cation titration data, while addition of Na^+ to the pre-incubated Tel22 sequence in the presence of 100 mM K^+ does not have any effect on the G-quadruplex conformation (Figure 7C and D). Therefore the multiple interconvertable G-quadruplex conformations of Tel22 associated with the K^+ ion are all indicated to be more stable than the basket-type Tel22 G-quadruplex associated with the Na^+ ion (Figure 10B). Unlike Tel26, conversion of the Na^+ form of Tel22 to its K^+ form is faster than can be detected by either CD or NMR (Figure 7C), and the related equilibrium occurs in minutes at a given Na^+/K^+ concentration ratio.

Our structure is in accord with other reported experimental data on the telomeric G-quadruplex structures

Because the K^+ structure is considered to be biologically more relevant due to the higher intracellular concentration of K^+, a number of biophysical and crosslinking studies have been reported in an attempt to characterize the telomeric G-quadruplex structure in K^+ solution (31,33–37,52). Our results are in accord with these reported experimental data.

Truncated telomeric DNA sequences lacking the 3′-flanking sequence were used in most of the reported studies. In a recent report by the Chaires group, a single substitution of 2-aminopurine (AP) was used for each of the adenine bases in the truncated Tel22 sequence (31). The order of the accessibility of 2-AP as probed by fluorescence quenching was found to be A13<A19<A1=A7 in K^+ solution. This is precisely as would be predicted based upon the hybrid-type G-quadruplex structure, i.e. the A1 (A3 of the Tel26 sequence) is the terminal residue and is exposed to solvent, while the A7 (A9 of Tel26) is located in the side loop and is also exposed to solvent. However, both the A13 (A15 of Tel26) and A19 (A21 of Tel26) are located in the lateral loops and are likely stacked with the neighboring G-tetrad and thus are less accessible. The different CD spectra reported in Na^+ and K^+ (32,33,37,52) are consistent with our results, while similar chemical reactivity patterns (37), similar platinum crosslinking patterns (36), and similar values of translational diffusion coefficients by photon correlation spectroscopy (32) of truncated telomeric sequences in the presence of Na^+ and K^+ are likely due to the co-existence of both structures in K^+ solution. In a recent report using ^{125}I-radioprobing experiments (34), the different DNA strand breakage probability observed only in the presence of K^+ but not Na^+ is also consistent with the hybrid-type G-quadruplex; i.e. the T(−2) (A1 in Tel26) is close to the ^{125}I-C18 (T20 in Tel26), while G14 (G16 in Tel26) is close to the ^{125}I-C(+1) (A25 in Tel26) in the hybrid-type G-quadruplex, which can thus be cleaved only in the presence of K^+.

Physiologically relevant conformation of the human telomeric sequence

Human telomeric DNA is typically 5–8 kb long with a 3′ single-stranded overhang of 100–200 nt consisting of tandem repeats of the sequence d(TTAGGG) (4,5). Telomerase is a cancer-specific reverse transcriptase that is activated in 80–85% of human tumor cells (15). The formation and stabilization of the G-quadruplex in the human telomeric sequence have been shown to inhibit the activity of telomerase, thus the telomeric DNA G-quadruplex has been considered as an attractive target for cancer therapeutic intervention (7,9,10,16–18). Structural information on the intact human telomeric G-quadruplex under physiologically relevant conditions is a prerequisite for structure-based rational drug design of G-quadruplex-interactive agents that specifically inhibit telomerase activity.

The hybrid-type G-quadruplex structure appears to be the physiologically relevant conformation of the human telomeric sequence. Significantly, the CD signature of the Tel26 and the wide-type telomeric sequence WT-Tel26 (Figure 2A) in K^+ solution are the same (Figure 3). The hybrid-type G-quadruplex structure is found to form readily in the presence of K^+, regardless of the presence of Na^+ (Figures 7 and 10). Moreover, the extended 26 nt telomeric sequence no longer forms a single stable G-quadruplex structure in the presence of Na^+, and the presence of K^+ readily converts the Na^+ conformation to the hybrid-type G-quadruplex conformation (Figures 7 and 10). Significantly,

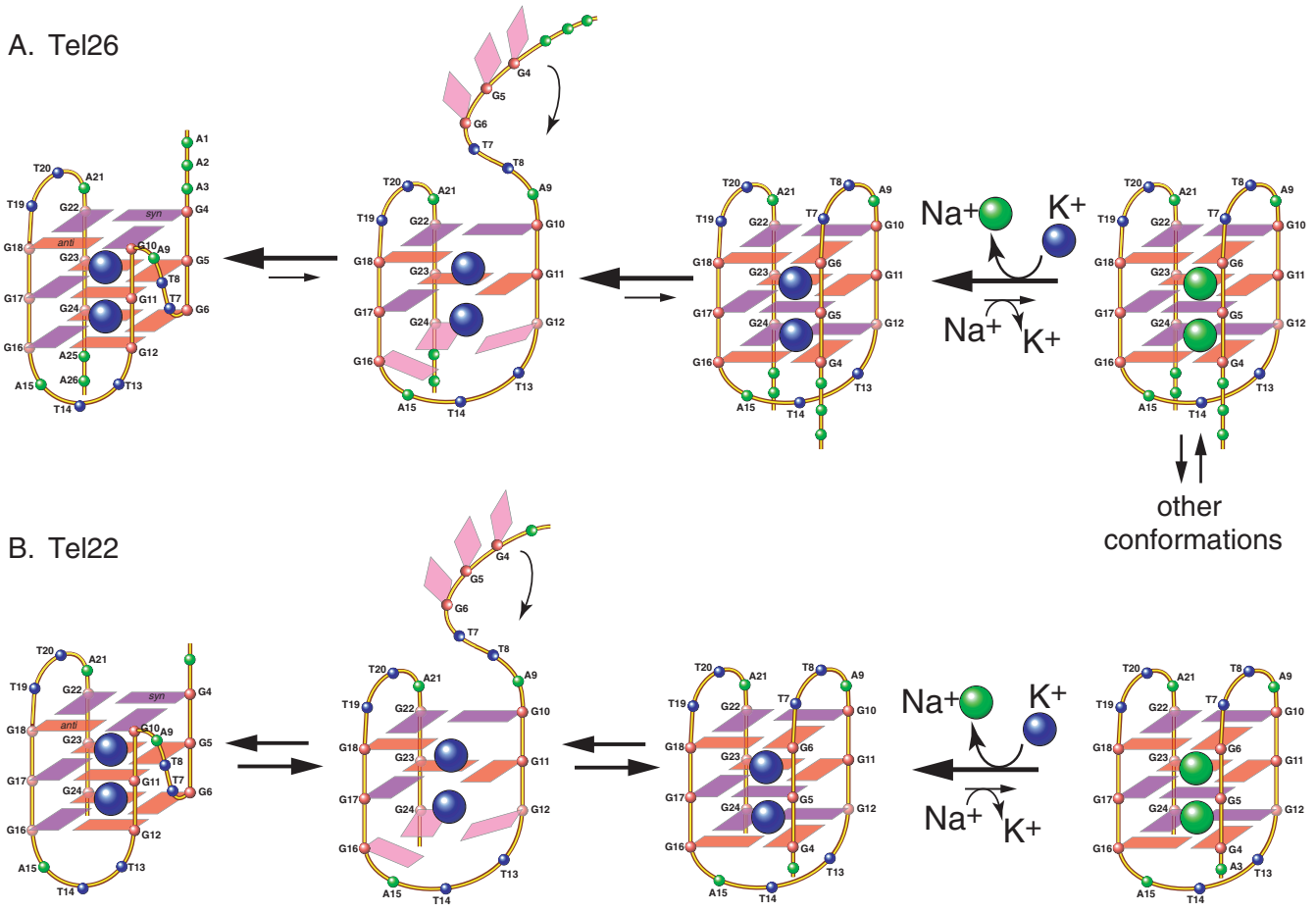

Figure 10. Schematic diagram of interconversions between the Na^+ and K^+ forms of telomeric G-quadruplexes. (**A**) For the extended four repeat telomeric sequence Tel26, the hybrid-type G-quadruplex structure is the most stable and thus the predominant form in the presence of K^+, regardless of the presence or absence of Na^+. Addition of K^+ readily converts the preformed Na^+-form G-quadruplex to the hybrid-type G-quadruplex conformation. Tel26 no longer forms a single stable intramolecular G-quadruplex structure in Na^+ solution, likely caused by the steric interference of the flanking sequences with the diagonal loop, both of which positioned on the same side of the basket-type G-quadruplex structure. (**B**) The truncated Tel22 forms a single stable basket-type intramolecular G-quadruplex in Na^+ solution. However, in the presence of K^+ Tel22 does not form a single G-quadruplex structure and is likely to have two stable G-quadruplex conformations co-existing. A possible mechanism of the interconversion of the two G-quadruplex conformations is proposed. The exchange rate between the two stable G-quadruplexes is slow on the NMR time scale at 25°C (Figure 2C). Addition of K^+ to the preformed Na^+ basket-type G-quadruplex readily converts the conformation to the K^+-form, thus the two interconvertable K^+ G-quadruplex conformations are both more stable than the Na^+-basket-type G-quadruplex.

the hybrid-type telomeric G-quadruplex adopts a novel and distinct folding topology, suggesting that it can be specifically targeted by G-quadruplex-interactive small molecule drugs.

Furthermore, the hybrid-type telomeric G-quadruplex structure reported in this article suggests a compact-stacking structure for multimers of this conformation in human telomeric DNA. The 5′ and 3′ ends of this hybrid-type telomeric G-quadruplex structure point in opposite directions, allowing the hybrid-type G-quadruplex to be readily folded and stacked end to end in the elongated linear telomeric DNA strand (Figure 11). Indeed, the adenines in the flanking sequence at each end of the Tel26 molecule are likely to mimic this stacking interaction and thus stabilize the G-quadruplex formation, as adenine residues have been shown to have greater stacking interactions than pyrimidines (42,47,59–62), probably owing to the extended aromatic ring system. In contrast, the basket-type G-quadruplex conformation appears to be less favored for a consecutive

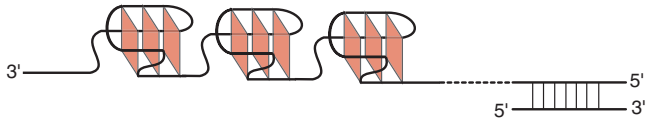

Figure 11. A schematic model of DNA secondary structure in human telomeres. The hybrid-type telomeric G-quadruplex structure reported in this article can be readily folded and stacked end to end to form a compact-stacking structure for multimers of this conformation in the elongated linear telomeric DNA strand.

packing on a linear telomeric DNA as its 5′ and 3′ ends as well as the diagonal loop all point in the same direction. Although the hybrid-type and parallel-type G-quadruplexes can both stack well in the extended telomeric sequence, the latter as suggested by Parkinson *et al.* (30), only the hybrid-type folding forms under physiological conditions in solution and is thus most likely to be of pharmacological relevance.

SUPPLEMENTARY DATA

Supplementary Data are available at NAR Online.

ACKNOWLEDGEMENTS

The authors thank the valuable communications and the technical help to Dr Laurence Hurley and his laboratory. We appreciate the technical help of Clemens Anklin from the Bruker Inc. on the JR-HMBC experiment. We also appreciate the technical help and the proofreading of the article by Dr Megan Carver. This research was supported by the National Institutes of Health (1K01CA83886 and 1S10 RR16659). Funding to pay the Open Access publication charges for this article was provided by NIH (1K01CA83886 and 1S10 RR16659) to DY.

Conflict of interest statement. None declared.

REFERENCES

1. Blackburn,E.H. (2000) Telomere states and cell fates. *Nature*, **408**, 53–56.
2. van Steensel,B., Smogorzewska,A. and de Lange,T. (1998) TRF2 protects human telomeres from end-to-end fusions. *Cell*, **92**, 401–413.
3. Hackett,J.A., Feldser,D.M. and Greider,C.W. (2001) Telomere dysfunction increases mutation rate and genomic instability. *Cell*, **106**, 275–286.
4. Makarov,V.L., Hirose,Y. and Langmore,J.P. (1997) Long G tails at both ends of human chromosomes suggest a C strand degradation mechanism for telomere shortening. *Cell*, **88**, 657–666.
5. McElligott,R. and Wellinger,R.J. (1997) The terminal DNA structure of mammalian chromosomes. *EMBO J.*, **16**, 3705–3714.
6. Harley,C.B., Futcher,A.B. and Greider,C.W. (1990) Telomeres shorten during aging of human fibroblasts. *Nature*, **345**, 458–460.
7. Mergny,J.L. and Helene,C. (1998) G-quadruplex DNA: a target for drug design. *Nature Med.*, **4**, 1366–1367.
8. Sun,D.Y. and Hurley,L.H. (2001) Targeting telomeres and telomerase. In Chaires,J.B. and Waring,M.J. (eds.), *METHODS IN ENZYMOLOGY, Drug-Nucleic Acid Interactions*. Academic Press Inc, San Diego, CA, vol. **340**, pp. 573–592.
9. Hurley,L.H. (2002) DNA and its associated processes as targets for cancer therapy. *Nature Rev. Cancer*, **2**, 188–200.
10. Neidle,S. and Parkinson,G. (2002) Telomere maintenance as a target for anticancer drug discovery. *Nature Rev. Drug Discov.*, **1**, 383–393.
11. Bodnar,A.G., Ouellette,M., Frolkis,M., Holt,S.E., Chiu,C.P., Morin,G.B., Harley,C.B., Shay,J.W., Lichtsteiner,S. and Wright,W.E. (1998) Extension of life-span by introduction of telomerase into normal human cells. *Science*, **279**, 349–352.
12. Harley,C.B. (1991) Telomere loss—mitotic clock or genetic time bomb. *Mutation Res.*, **256**, 271–282.
13. Sun,H., Karow,J.K., Hickson,I.D. and Maizels,N. (1998) The Bloom's Syndrome helicase unwinds G4 DNA. *J. Biol. Chem.*, **273**, 27587–27592.
14. Sun,H., Bennett,R.J. and Maizels,N. (1999) The *Saccharomyces cerevisiae* Sgs1 helicase efficiently unwinds G–G paired DNAs. *Nucleic Acids Res.*, **27**, 1978–1984.
15. Healy,K.C. (1995) Telomere dynamics and telomerase activation in tumor progression—prospects for prognosis and therapy. *Oncol. Res.*, **7**, 121–130.
16. Hurley,L.H. (2001) Secondary DNA structures as molecular targets for cancer therapeutics. *Biochem. Soc. Trans.*, **29**, 692–696.
17. Hurley,L.H., Wheelhouse,R.T., Sun,D., Kerwin,S.M., Salazar,M., Fedoroff,O.Y., Han,F.X., Han,H.Y., Izbicka,E. and Von Hoff,D.D. (2000) G-quadruplexes as targets for drug design. *Pharmacol. Ther.*, **85**, 141–158.
18. Neidle,S. and Read,M.A. (2000) G-quadruplexes as therapeutic targets. *Biopolymers*, **56**, 195–208.
19. Simonsson,T., Pecinka,P. and Kubista,M. (1998) DNA tetraplex formation in the control region of c-myc. *Nucleic Acids. Res.*, **26**, 1167–1172.
20. Siddiqui-Jain,A., Grand,C.L., Bearss,D.J. and Hurley,L.H. (2002) Direct evidence for a G-quadruplex in a promoter region and its targeting with a small molecule to repress c-MYC transcription. *Proc. Natl Acad. Sci. USA*, **99**, 11593–11598.
21. Etzioni,S., Yafe,A., Khateb,S., Weisman-Shomer,P., Bengal,E. and Fry,M. (2005) Homodimeric MyoD preferentially binds tetraplex structures of regulatory sequences of muscle-specific genes. *J. Biol. Chem.*, **280**, 26805–26812.
22. Yafe,A., Etzioni,S., Weisman-Shomer,P. and Fry,M. (2005) Formation and properties of hairpin and tetraplex structures of guanine-rich regulatory sequences of muscle-specific genes. *Nucleic Acids Res.*, **33**, 2887–2900.
23. Lew,A., Rutter,W.J. and Kennedy,G.C. (2000) Unusual DNA structure of the diabetes susceptibility locus IDDM2 and its effect on transcription by the insulin promoter factor Pur-1/MAZ. *Proc. Natl Acad. Sci. USA*, **97**, 12508–12512.
24. Hammondkosack,M.C.U., Dobrinski,B., Lurz,R., Docherty,K. and Kilpatrick,M.W. (1992) The human insulin gene linked polymorphic region exhibits an altered DNA-structure. *Nucleic Acids Res.*, **20**, 231–236.
25. Howell,R.M., Woodford,K.J., Weitzmann,M.N. and Usdin,K. (1996) The chicken beta-globin gene promoter forms a novel 'cinched' tetrahelical structure. *J. Biol. Chem.*, **271**, 5208–5214.
26. Rankin,S., Reszka,A.P., Huppert,J., Zloh,M., Parkinson,G.N., Todd,A.K., Ladame,S., Balasubramanian,S. and Neidle,S. (2005) Putative DNA quadruplex formation within the human c-kit oncogene. *J. Am. Chem. Soc.*, **127**, 10584–10589.
27. Cogoi,S., Quadrifoglio,F. and Xodo,L.E. (2004) G-rich oligonucleotide inhibits the binding of a nuclear protein to the Ki-ras promoter and strongly reduces cell growth in human carcinoma pancreatic cells. *Biochemistry*, **43**, 2512–2523.
28. Sun,D.Y., Pourpak,A., Beetz,K. and Hurley,L.H. (2003) Direct evidence for the formation of G-quadruplex in the proximal promoter region of the RET protooncogene and its targeting with a small molecule to repress RET protooncogene transcription. *Clin. Cancer Res.*, **9**, 6122S–6123S.
29. Wang,Y. and Patel,D.J. (1993) Solution structure of the human telomeric repeat $D[Ag_3(T_2Ag_3)_3]$ G-tetraplex. *Structure*, **1**, 263–282.
30. Parkinson,G.N., Lee,M.P.H. and Neidle,S. (2002) Crystal structure of parallel quadruplexes from human telomeric DNA. *Nature*, **417**, 876–880.
31. Li,J., Correia,J.J., Wang,L., Trent,J.O. and Chaires,J.B. (2005) Not so crystal clear: the structure of the human telomere G-quadruplex in solution differs from that present in a crystal. *Nucleic Acids Res.*, **33**, 4649–4659.
32. Wlodarczyk,A., Grzybowski,P., Patkowski,A. and Dobek,A. (2005) Effect of ions on the polymorphism, effective charge, and stability of human telomeric DNA. Photon correlation spectroscopy and circular dichroism studies. *J. Phys. Chem. B*, **109**, 3594–3605.
33. Qi,J.Y. and Shafer,R.H. (2005) Covalent ligation studies on the human telomere quadruplex. *Nucleic Acids Res.*, **33**, 3185–3192.
34. He,Y.J., Neumann,R.D. and Panyutin,I.G. (2004) Intramolecular quadruplex conformation of human telomeric DNA assessed with I-125-radioprobing. *Nucleic Acids Res.*, **32**, 5359–5367.
35. Ying,L.M., Green,J.J., Li,H.T., Klenerman,D. and Balasubramanian,S. (2003) Studies on the structure and dynamics of the human telomeric G-quadruplex by single-molecule fluorescence resonance energy transfer. *Proc. Natl Acad. Sci. USA*, **100**, 14629–14634.
36. Redon,S., Bombard,S., Elizondo-Riojas,M.A. and Chottard,J.C. (2003) Platinum cross-linking of adenines and guanines on the quadruplex structures of the $AG_3(T_2AG_3)_3$ and $(T_2AG_3)_4$ human telomere sequences in Na^+ and K^+ solutions. *Nucleic Acids Res.*, **31**, 1605–1613.
37. Balagurumoorthy,P. and Brahmachari,S.K. (1994) Structure and stability of human telomeric sequence. *J. Biol. Chem.*, **269**, 21858–21869.
38. Phan,A.T. and Patel,D.J. (2003) Two-repeat human telomeric d(TAGGGTTAGGGT) sequence forms interconverting parallel and antiparallel G-quadruplexes in solution: distinct topologies, thermodynamic properties, and folding/unfolding kinetics. *J. Am. Chem. Soc.*, **125**, 15021–15027.
39. Zhang,N., Phan,A.T. and Patel,D.J. (2005) (3+1) Assembly of three human telomeric repeats into an asymmetric dimeric G-quadruplex. *J. Am. Chem. Soc.*, **127**, 17277–17285.

40. Dai,J., Dexheimer,T.S., Chen,D., Carver,M., Ambrus,A., Jones,R.A. and Yang,D. (2006) An intramolecular G-quadruplex structure with mixed parallel/antiparallel G-strands formed in the human BCL-2 promoter region in solution. *J. Am. Chem. Soc.*, **128**, 1096–1098.
41. Dai,J.X., Punchihewa,C., Mistry,P., Ooi,A.T. and Yang,D.Z. (2004) Novel DNA *bis*-intercalation by MLN944, a potent clinical bisphenazine anticancer drug. *J. Biol. Chem.*, **279**, 46096–46103.
42. Ambrus,A., Chen,D., Dai,J.X., Jones,R.A. and Yang,D.Z. (2005) Solution structure of the biologically relevant G-quadruplex element in the human c-MYC promoter. implications for G-quadruplex stabilization. *Biochemistry*, **44**, 2048–2058.
43. Zhao,H., Pagano,A.R., Wang,W.M., Shallop,A., Gaffney,B.L. and Jones,R.A. (1997) Use of a C-13 atom to differentiate two N-15-labeled nucleosides. Syntheses of [(NH_2)-N-15]-adenosine, [1,NH_2-N-15(2)]- and [2-C-13-1,NH_2-N-15(2)]-guanosine, and [1,7,NH_2-N-15(3)]- and [2-C-13-1,7,NH_2-N-15(3)]-2′-deoxyguanosine. *J. Org. Chem.*, **62**, 7832–7835.
44. Plateau,P. and Gueron,M. (1982) Exchangeable proton NMR without base-line distortion, using new strong-pulse sequences. *J. Am. Chem. Soc.*, **104**, 7310–7311.
45. Phan,A.T., Gueron,M. and Leroy,J.L. (2001) *Nuclear Magnetic Resonance of Biologica Macromolecules, Pt A*. Academic Press Inc., San Diego, CA, vol. **338**, pp. 341–371.
46. Phan,A.T. (2000) Long-range imino proton-C-13 J-couplings and the through-bond correlation of imino and non-exchangeable protons in unlabeled DNA. *J. Biomol. NMR*, **16**, 175–178.
47. Phan,A.T., Modi,Y.S. and Patel,D.J. (2004) Propeller-type parallel-stranded G-quadruplexes in the human c-myc promoter. *J. Am. Chem. Soc.*, **126**, 8710–8716.
48. Dapic,V., Abdomerovic,V., Marrington,R., Peberdy,J., Rodger,A., Trent,J.O. and Bates,P.J. (2003) Biophysical and biological properties of quadruplex oligodeoxyribonucleotides. *Nucleic Acids. Res.*, **31**, 2097–2107.
49. Kypr,J., Fialova,M., Chladkova,J., Tumova,M. and Vorlickova,M. (2001) Conserved guanine-guanine stacking in tetraplex and duplex DNA. *Eur. Biophys. J. Biophys. Lett.*, **30**, 555–558.
50. Seenisamy,J., Rezler,E.M., Powell,T.J., Tye,D., Gokhale,V., Joshi,C.S., Siddiqui-Jain,A. and Hurley,L.H. (2004) The dynamic character of the G-quadruplex element in the c-MYC promoter and modification by TMPyP4. *J. Am. Chem. Soc.*, **126**, 8702–8709.
51. Schultze,P., Macaya,R.F. and Feigon,J. (1994) Three-dimensional solution structure of the thrombin-binding DNA aptamer d(GGTTGGTGTGGTTGG). *J. Mol. Biol.*, **235**, 1532–1547.
52. Rezler,E.M., Seenisamy,J., Bashyam,S., Kim,M.Y., White,E., Wilson,W.D. and Hurley,L.H. (2005) Telomestatin and diseleno sapphyrin bind selectively to two different forms of the human telomeric G-quadruplex structure. *J. Am. Chem. Soc.*, **127**, 9439–9447.
53. Wang,Y. and Patel,D.J. (1994) Solution structure of the *Tetrahymena* telomeric repeat D(T(2)G(4))(4) G-tetraplex. *Structure*, **2**, 1141–1156.
54. Sun,D.Y., Guo,K.X., Rusche,J.J. and Hurley,L.H. (2005) Facilitation of a structural transition in the polypurine/polypyrimidine tract within the proximal promoter region of the human VEGF gene by the presence of potassium and G-quadruplex-interactive agents. *Nucleic Acids Res.*, **33**, 6070–6080.
55. De Armond,R., Wood,S., Sun,D.Y., Hurley,L.H. and Ebbinghaus,S.W. (2005) Evidence for the presence of a guanine quadruplex forming region within a polypurine tract of the hypoxia inducible factor 1 alpha promoter. *Biochemistry*, **44**, 16341–16350.
56. Hazel,P., Huppert,J., Balasubramanian,S. and Neidle,S. (2004) Loop-length-dependent folding of G-quadruplexes. *J. Am. Chem. Soc.*, **126**, 16405–16415.
57. Wang,Y. and Patel,D.J. (1995) Solution structure of the oxytricha telomeric repeat d[G4(T4G4)3] G-tetraplex. *J. Mol. Biol.*, **251**, 76–94.
58. Vorlickova,M., Kejnovska,I., Tumova,M. and Kypr,J. (2001) Conformational properties of DNA fragments containing GAC trinucleotide repeats associated with skeletal displasias. *Eur. Biophys. J. Biophys. Lett.*, **30**, 179–185.
59. Matsugami,A., Ouhashi,K., Kanagawa,M., Liu,H., Kanagawa,S., Uesugi,S. and Katahira,M. (2001) An intramolecular quadruplex of (GGA)4 triplet repeat DNA with a G:G:G:G tetrad and a G(:A):G(:A):G(:A):G heptad, and its dimeric interaction. *J. Mol. Biol.*, **313**, 255–269.
60. Matsugami,A., Okuizumi,T., Uesugi,S. and Katahira,M. (2003) Intramolecular higher order packing of parallel quadruplexes comprising a G:G:G:G tetrad and a G(:A):G(:A):G(:A):G heptad of GGA triplet repeat DNA. *J. Biol. Chem.*, **278**, 28147–28153.
61. Kettani,A., Gorin,A., Majumdar,A., Hermann,T., Skripkin,E., Zhao,H., Jones,R. and Patel,D.J. (2000) A dimeric DNA interface stabilized by stacked A.(G.G.G.G). A hexads and coordinated monovalent cations. *J. Mol. Biol.*, **297**, 627–644.
62. Kuryavyi,V., Kettani,A., Wang,W.M., Jones,R. and Patel,D.J. (2000) A diamond-shaped zipper-like DNA architecture containing triads sandwiched between mismatches and tetrads. *J. Mol. Biol.*, **295**, 455–469.